Time evolution of the radial perturbations and linear stability of solitons and black holes in a generalized Skyrme model

Daniela D. Doneva,[1,2,*] Kostas D. Kokkotas,[2,†] Ivan Zh. Stefanov,[3,‡] and Stoytcho S. Yazadjiev[4,§]

[1]*Department of Astronomy, Faculty of Physics, St. Kliment Ohridski University of Sofia,*
5, James Bourchier Boulevard, 1164 Sofia, Bulgaria
[2]*Theoretical Astrophysics, Eberhard-Karls University of Tübingen, Tübingen 72076, Germany*
[3]*Department of Applied Physics, Technical University of Sofia, 8, Kliment Ohridski Boulevard, 1000 Sofia, Bulgaria*
[4]*Department of Theoretical Physics, Faculty of Physics, St. Kliment Ohridski University of Sofia,*
5, James Bourchier Boulevard, 1164 Sofia, Bulgaria
(Received 8 August 2011; published 12 October 2011)

We study the time evolution of the radial perturbation for self-gravitating soliton and black-hole solutions in a generalized Skyrme model in which a dilaton is present. The background solutions were obtained recently by some of the authors. For both the solitons and the black holes two branches of solutions exist which merge at some critical value of the corresponding parameter. The results show that, similar to the case without a scalar field, one of the branches is stable against radial perturbations and the other is unstable. The conclusions for the linear stability of the black holes in the generalized Skyrme model are also in agreement with the results from the thermodynamical stability analysis based on the turning point method.

I. INTRODUCTION

Our intuition for the properties of the solutions describing self-gravitating objects in general relativity is based, to a large extent, on some exact solutions which belong to the Kerr-Newman class of black holes. For these solutions uniqueness theorems, and theorems stating that globally regular self-gravitating solutions (solitons) do not exist, have been proven rigorously in the case of vacuum or linear matter models such as Maxwell electrodynamics [1–5]. As the investigations in the last two decades revealed, the standard intuition often fails when nonlinear matter models are considered [6], which makes the study of self-gravitating solutions in such models vital for fundamental physics.

One of the effective nonlinear matter models which has attracted much attention is Skyrme's theory [7,8]. In this theory baryons are described as solitons in an effective theory of mesons. The interest in Skyrme theory was revived in the 1980s when it was found that the Skyrme Lagrangian can be derived from QCD in the low-energy regime.

Self-gravitating solutions in Skyrme theory were considered for the first time by Luckock *et al.* [9]. The solutions in Einstein-Skyrme (ES) theory are nonunique, and those with a nontrivial Skyrme field can be divided into two branches. The first branch of solutions has a well-defined flat-space limit. It was obtained by Droz, Heusler, and Straumann [10]. The authors found that these solutions

are stable against spherically symmetric perturbations [11,12]. The second branch of solutions was discovered by Bizon and Chmaj soon after that [13]. This branch has no flat-space limit and it is unstable, as the authors' analysis revealed. The stability of the ES solitons has also been studied in [14–16]. There is also a branch of solutions that has a trivial Skyrme field and coincides with the pure Schwarzschild black hole. Self-gravitating solutions in Skyrme theory, both black holes and solitons, have also been studied in a series of papers [17–27].

Different modifications of Skyrme theory have been considered in order to cure some of its deficiencies which are present in the original version of the theory [7]. One possible generalization is the inclusion of a dilaton. The dilaton is added in the theory to restore scale invariance which is also characteristic for the underlying QCD. It has also been considered as a source of additional intermediate-range attractive forces which are vital for the formation of stable multisoliton configurations such as nuclei and baryon stars. A generalized Skyrme model (GSM) which includes a dilaton has been derived from QCD in the low-energy regime in [28–30]. In a recent paper [31] we reported numerical solutions describing self-gravitating solitons and black holes in the GSM. They are generalizations of the soliton and black-hole solutions that have been obtained numerically in [10,13].

The aim of the current paper is to study the response of the self-gravitating GSM solutions [31], both soliton and black-hole types, to small radial perturbations and, in particular, to determine if the inclusion of the dilaton in Skyrme theory changes the stability properties. We study the quasinormal modes (QNMs) of the solutions by evolving the time-dependent wave equations.

*ddoneva@phys.uni-sofia.bg
†kostas.kokkotas@uni-tuebingen.de
‡izhivkov@tu-sofia.bg
§yazad@phys.uni-sofia.bg

The problem of studying the QNMs and the stability of the GSM solutions is mathematically more complex than that of the ES solutions since in the former case a system of two coupled wave equations for the perturbations of the Skyrme field and the dilaton has to be solved even though the considerations are restricted to radial perturbations (in the ES case the problem is reduced to only one wave equation for the Skyrme field). What makes the problem even more difficult is that the wave equation for the per-turbations of the dilaton contains a potential which is not vanishing at infinity; i.e. the scalar field is massive and the time evolution of the perturbations has some specific prop-erties [32–38].

The paper is organized as follows. The GSM coupled to gravity is briefly presented in Sec. II. In this section the time-dependent field equations are given. The system of coupled equations for the radial part of the perturbations of the Skyrme field and the dilaton is derived in Sec. III and solved with the proper boundary conditions numerically in Sec. IV. In Sec. V a summary of the results is given.

II. THE GENERALIZED SKYRME MODEL

A. Action

Let us briefly introduce the model considered in [31]. We start with the following action:

$$S = \int d^4x \sqrt{-g}\left(-\frac{R}{16\pi G} + L_M\right). \tag{1}$$

The flat-space Lagrangian of the GSM can be found in [30]. When gravity is included the GSM Lagrangian is naturally generalized to the form

$$
\begin{aligned}
L_M = &\frac{1}{4}f_\pi^2 \exp(-2\sigma)\,\mathrm{Tr}[\nabla_\mu U \nabla^\mu U^+] \\
&+ \frac{N_f f_\pi^2}{4}\exp(-2\sigma)g^{\mu\nu}\partial_\mu\sigma\partial_\nu\sigma \\
&+ \frac{1}{32e^2}\,\mathrm{Tr}[(\nabla_\mu U)U^+, (\nabla_\nu U)U^+]^2 + V_{\mathrm{GSM}}(\sigma),
\end{aligned}
\tag{2}
$$

where the derivatives have been substituted with covariant derivatives. Here U is the SU(2) chiral field, σ is the dilaton, ∇_μ is the covariant derivative with respect to the metric $g_{\mu\nu}$, f_π is the pion decay constant, e is the Skyrme constant, C_g is the gluon condensate, N_f is the number of flavors, and $\varepsilon = 8N_f/(33 - 2N_f)$. The first two terms in (2) are the kinetic terms for the chiral and the dilaton fields. The third term is the one introduced by Skyrme for the stabilization of the soliton solutions. The potential of the dilaton field is given by

$$V_{\mathrm{GSM}}(\sigma) = -\frac{C_g N_f}{48}\left[\exp(-4\sigma) - 1 + \frac{4}{\varepsilon}(1 - \exp(-\varepsilon\sigma))\right]. \tag{3}$$

The dilaton couples only to those terms of Lagrangian density that break the scale invariance.[1]

Instead of σ it is more convenient to work with the function Φ which is defined by

$$\Phi = \exp(-\sigma). \tag{4}$$

B. Reduced Lagrangian

We are going to restrict our considerations to the spheri-cally symmetric case. In [31] the hedgehog ansatz for the chiral field

$$U = \exp[\boldsymbol{\tau}\cdot\hat{\mathbf{r}}F(r, t)] \tag{5}$$

was chosen. Here $\boldsymbol{\tau}$ are the Pauli matrices and $\hat{\mathbf{r}}$ is a unit radial vector. With the following time-dependent ansatz for the metric,

$$ds^2 = e^{\chi(t,r)}dt^2 - e^{\alpha(t,r)}dr^2 - r^2(d\theta^2 + \sin^2\theta d\varphi^2), \tag{6}$$

the Lagrangian (2) takes the form[2]

$$
\begin{aligned}
L_m = \frac{a^2}{b}\Bigg[&\frac{u}{x^2}(e^{-\chi}\dot{F}^2 - e^{-\alpha}F'^2) - \frac{v}{x^2} \\
&+ \tilde{N}(e^{-\chi}\dot{\Phi}^2 - e^{-\alpha}\Phi'^2) + \frac{1}{a}\tilde{V}\Bigg],
\end{aligned}
\tag{7}
$$

where

$$u = x^2\Phi^2 + 2\sin^2 F, \qquad v = \left(2\Phi^2 + \frac{\sin^2 F}{x^2}\right)\sin^2 F, \tag{8}$$

$$\tilde{V}(\Phi) = \frac{16\pi Gb}{a}V_{\mathrm{GSM}}(\Phi) = -\frac{\gamma\tilde{N}b}{a}\left[\Phi^4 - 1 + \frac{4}{\varepsilon}(1 - \Phi^\varepsilon)\right]. \tag{9}$$

We have introduced the following constants:

$$a = 8\pi G f_\pi^2, \quad b = 8\pi G\frac{1}{e^2}, \quad \gamma = 2\pi G\frac{C_g}{3}, \quad \tilde{N} = \frac{N_f}{2}, \tag{10}$$

and dimensionless variables $\tau = ef_\pi t$, $x = ef_\pi r$. The de-rivative with respect to the dimensionless time coordinate τ is denoted by a dot, while the derivative with respect to the dimensionless radial coordinate x is denoted by a prime. Below we will also use the parameter[3]

$$D_{\mathrm{eff}} = \frac{\gamma\tilde{N}}{2ae^2f_\pi^2}. \tag{11}$$

---

[1]For more details we refer the reader to [31].
[2]The notation we choose here is slightly different from that in [31]. It facilitates the comparison of the equations and the results to the ES case [10–13].
[3]The parameter a is 2 times bigger that the parameter α used in [10–13], and the parameter D_{eff} is chosen to be the same as in [30].

For the number of flavors, we fixed the value $N_f = 2$, so $\tilde{N} = 1$.

C. Time-dependent field equations

The Einstein equations have the following form:

$$G_{\mu\nu} = -\tfrac{1}{2}T_{\mu\nu}, \tag{12}$$

$$T_{\mu\nu} = -g_{\mu\nu}L_m + 2\frac{\delta L_m}{\delta g^{\mu\nu}}. \tag{13}$$

The (tt), (rr), and (tr) components of (12) are

$$[e^{-\alpha}(1 - x\alpha') - 1] = -a(\tfrac{1}{2}uw + \tfrac{1}{2}v + \tfrac{1}{2}x^2 z) + \tfrac{1}{2}x^2 \tilde{V}, \tag{14}$$

$$[e^{-\alpha}(1 + x\chi') - 1] = a(\tfrac{1}{2}uw - \tfrac{1}{2}v + \tfrac{1}{2}x^2 z) + \tfrac{1}{2}x^2 \tilde{V}, \tag{15}$$

$$\dot{\alpha} = \frac{a}{x}(u\dot{F}F' + x^2\tilde{N}\dot{\Phi}\,\Phi'), \tag{16}$$

where

$$w = e^{-\chi}\dot{F}^2 + e^{-\alpha}F'^2, \tag{17}$$

$$z = \tilde{N}(e^{-\chi}\dot{\Phi}^2 + e^{-\alpha}\Phi'^2). \tag{18}$$

The combination of Eqs. (14) and (15) gives the following useful expression:

$$\frac{\chi' - \alpha'}{2} = \frac{e^\alpha}{x}\left(1 - \frac{1}{2}av + \frac{1}{2}x^2\tilde{V}\right) - \frac{1}{x}. \tag{19}$$

The time-dependent field equations for F and Φ obtained from (7) are

$$e^{\alpha-\chi}\left[\frac{\dot{\alpha} - \dot{\chi}}{2}u\dot{F} + (u\dot{F})^{\cdot}\right]$$
$$= \left[\frac{\chi' - \alpha'}{2}uF' + (uF')'\right] + \frac{1}{2}u_F(e^{\alpha-\chi}\dot{F}^2 - F'^2)$$
$$- \frac{1}{2}e^\alpha v_F = 0, \tag{20}$$

$$e^{\alpha-\chi}\left[\frac{\dot{\alpha} - \dot{\chi}}{2}x^2\dot{\Phi} + (x^2\dot{\Phi})^{\cdot}\right]$$
$$= \left[\frac{\chi' - \alpha'}{2}x^2\Phi' + (x^2\Phi')'\right] + \frac{1}{2\tilde{N}}u_\Phi(e^{\alpha-\chi}\dot{F}^2 - F'^2)$$
$$- \frac{1}{2\tilde{N}}e^\alpha v_\Phi + \frac{x^2}{2a\tilde{N}}e^\alpha\tilde{V}_\Phi = 0, \tag{21}$$

where $(\ldots)_\Phi$ denotes the partial derivative with respect to Φ, and $(\ldots)_F$ denotes the partial derivative with respect to F.

III. EQUATIONS FOR THE RADIAL PERTURBATIONS

We reduce our considerations to radial perturbations

$$\alpha(\tau,x) = \alpha_0(x) + \delta\alpha(\tau,x), \quad \chi(\tau,x) = \chi_0(x) + \delta\chi(\tau,x),$$
$$F(\tau,x) = F_0(x) + \delta F(\tau,x), \quad \Phi(\tau,x) = \Phi_0(x) + \delta\Phi(\tau,x),$$

and follow the scheme presented in [11]. It turns out that the evolution of the Skyrme field and the scalar field perturbations, δF and $\delta\Phi$, respectively, can be studied independently from the perturbations of the metric. The equation for δF, obtained from (20), is

$$e^{\alpha_0 - \chi_0}u_0\ddot{\delta F}$$
$$= u_0\delta F'' + \left(\frac{\chi_0' - \alpha_0'}{2}u_0 + u_0'\right)\delta F' + u_{0\Phi}F_0'\delta\Phi'$$
$$+ u_{0\Phi}'F_0'\delta\Phi + \left(F_0'' + \frac{\chi_0' - \alpha_0'}{2}F_0'\right)\delta u + u_{0F}'F_0'\delta F$$
$$- \frac{1}{2}F_0'^2\delta u_F - \frac{1}{2}e^{\alpha_0}\delta v_F - \frac{1}{2}e^{\alpha_0}v_{0F}\delta\alpha + u_0F_0'\frac{\delta\chi' - \delta\alpha'}{2}. \tag{22}$$

From (21) we obtain the following equation for the perturbations of the scalar field $\delta\Phi$:

$$e^{\alpha_0 - \chi_0}x^2\ddot{\delta\Phi}$$
$$= x^2\delta\Phi'' + \left(\frac{\chi_0' - \alpha_0'}{2}x^2 + 2x\right)\delta\Phi' - \frac{1}{\tilde{N}}u_{0\Phi}F_0'\delta F'$$
$$- \frac{1}{2\tilde{N}}F_0'^2\delta u_\Phi + \frac{1}{2\tilde{N}}e^{\alpha_0}\left(-\delta v_\Phi + \frac{x^2}{a}\delta\tilde{V}_\Phi\right)$$
$$+ \frac{1}{2\tilde{N}}e^{\alpha_0}\left(-v_{0\Phi} + \frac{x^2}{a}\tilde{V}_{0\Phi}\right)\delta\alpha + x^2\Phi_0'\frac{\delta\chi' - \delta\alpha'}{2}, \tag{23}$$

where

$$\delta u = u_{0F}\delta F + u_{0\Phi}\delta\Phi, \qquad \delta v = v_{0F}\delta F + v_{0\Phi}\delta\Phi,$$
$$\delta u_F = u_{0FF}\delta F + u_{0F\Phi}\delta\Phi, \quad \delta v_F = v_{0FF}\delta F + v_{0F\Phi}\delta\Phi,$$
$$\delta u_\Phi = u_{0\Phi F}\delta F + u_{0\Phi\Phi}\delta\Phi, \quad \delta v_\Phi = v_{0\Phi F}\delta F + v_{0\Phi\Phi}\delta\Phi,$$
$$\delta\tilde{V}_\Phi = \tilde{V}_{0\Phi\Phi}\delta\Phi.$$

Throughout the paper, the lower index $(\ldots)_0$ means that the corresponding quantity refers to the background static solution. Lower indices F and Φ denote the corresponding partial derivatives. The variation of Eq. (16) gives

$$\dot{\delta\alpha} = \frac{a}{x}(u_0F_0'\dot{\delta F} + x^2\tilde{N}\Phi_0'\dot{\delta\Phi}). \tag{24}$$

The integration of the above expression with respect to τ gives

$$\delta\alpha = \frac{a}{x}(u_0F_0'\delta F + x^2\tilde{N}\Phi_0'\delta\Phi) \tag{25}$$

and it allows us to relate the perturbations of the metric functions $\delta\alpha$ to the perturbations of the matter fields δF and $\delta\Phi$. Another useful relation can be obtained from (19),

$$\frac{\delta\chi' - \delta\alpha'}{2} = \frac{e^{\alpha_0}}{x}\left[\left(1 - \frac{1}{2}av_0 + \frac{1}{2}x^2\tilde{V}_0\right)\delta\alpha - \frac{1}{2}a\delta v + \frac{1}{2}x^2\delta\tilde{V}\right]. \tag{26}$$

Relations (25) and (26), substituted back into (22) and (23), allow us to exclude the variations of the metric and to

obtain a system of two coupled equations (each of them of second order) for δF and $\delta \Phi$.

By the following substitution,

$$\delta F = \frac{\zeta}{\sqrt{u_0}}, \qquad \delta \Phi = \frac{\Psi}{x}, \qquad (27)$$

we obtain a system of coupled wave equations

$$- e^{\alpha_0 - \chi_0} \ddot{\zeta} + \zeta'' + \frac{\chi_0' - \alpha_0'}{2} \zeta' + A_1 \zeta + A_2 \Psi' + A_3 \Psi = 0, \qquad (28)$$

$$- e^{\alpha_0 - \chi_0} \ddot{\Psi} + \Psi'' + \frac{\chi_0' - \alpha_0'}{2} \Psi' + B_1 \Psi + B_2 \zeta' + B_3 \zeta = 0. \qquad (29)$$

The coefficients A_1, A_2, A_3, B_1, B_2, and B_3 are given in the Appendix. If we multiply (28) and (29) by $e^{\chi_0 - \alpha_0}$ and introduce a new radial coordinate

$$dx_* = \frac{dx}{e^{(\chi_0 - \alpha_0)/2}}, \qquad (30)$$

the system of equations takes the form

$$- \frac{\partial^2 \zeta}{\partial \tau^2} + \frac{\partial^2 \zeta}{\partial x_*^2} + \tilde{A}_1 \zeta + \tilde{A}_2 \frac{\partial \Psi}{\partial x_*} + \tilde{A}_3 \Psi = 0, \qquad (31)$$

$$- \frac{\partial^2 \Psi}{\partial \tau^2} + \frac{\partial^2 \Psi}{\partial x_*^2} + \tilde{B}_1 \Psi + \tilde{B}_2 \frac{\partial \zeta}{\partial x_*} + \tilde{B}_3 \zeta = 0. \qquad (32)$$

The coefficients $\tilde{A}_1$, $\tilde{A}_2$, $\tilde{A}_3$, $\tilde{B}_1$, $\tilde{B}_2$, and $\tilde{B}_3$ are given in the Appendix.

Let us describe the qualitative properties of the wave equations. If we had one wave equation (which could be transformed to a stationary Schrödinger-like equation by a proper separation of the time and spatial variables) the QNM frequencies would depend strongly on the shape of the potential. In our case we have two coupled wave equations and the notion of potential is not so clear. Still, the coefficients in front of the zeroth order derivatives of the wave functions, $\tilde{A}_1$ and $\tilde{B}_1$, respectively, determine the properties of the solutions. Thus we introduce two functions U^ζ and U^Ψ which can be expressed by $\tilde{A}_1$ and $\tilde{B}_1$ and which we will call potentials of the wave equations for ζ and Ψ, respectively. As the results show, the presence of unstable modes (solutions divergent with time) depends on whether these potentials have a deep enough negative minimum.

The potentials U^ζ and U^Ψ for the solitons are defined as

$$U^\zeta = -e^{\chi_0 - \alpha_0} \left(A_1 - \frac{2}{x^2} \right) = -\left(\tilde{A}_1 - \frac{2e^{\chi_0 - \alpha_0}}{x^2} \right), \quad U^\Psi = -\tilde{B}_1, \qquad (33)$$

where U^ζ is chosen in such a way that it is regular at the origin (see [11] for a more detailed discussion on that definition) and U^Ψ is also finite at $x = 0$. The potentials for the black-hole solutions are simply

$$U^\zeta = -\tilde{A}_1, \qquad U^\Psi = -\tilde{B}_1, \qquad (34)$$

where both U^ζ and U^Ψ are zero on the event horizon x_H.

It is also important to comment on the asymptotic value of the potentials at infinity. For both the black holes and the solitons, U^ζ tends to zero when $x \to \infty$, but U^Ψ has a nonzero value at infinity. The reason is that the scalar field we are considering is massive because of the specific form of the potential $\tilde{V}(\Phi)$, defined by Eq. (3). The mass m of the scalar field can be defined through the asymptotic value of the potential U^Ψ, i.e. as

$$\lim_{x \to \infty} U^\Psi = -m^2. \qquad (35)$$

Using Eq. (23) it can be easily derived that

$$\lim_{x \to \infty} \left(\frac{\tilde{V}_{0\Phi\Phi}}{2\tilde{N}a} \right) = -m^2. \qquad (36)$$

One of the main differences in the time evolution of a massive test scalar field in comparison to the massless case is that the tail is oscillating with the period [32]

$$T = \frac{2\pi}{m}. \qquad (37)$$

In the limit $m \to 0$ the oscillations of the tail disappear and we are left with the standard power law tail. Even though in our problem we are dealing with two wave equations—one for the Skyrme field and one for the massive scalar field—it is expected (and confirmed by the numerical results) that the tail will again be oscillatory with period (37).

Another point worth mentioning is the qualitative behavior of the QNM frequencies for the stable and the unstable modes. As it is well known, the frequencies of the stable modes are complex, where the real part is inversely proportional to the period of the oscillations and the imaginary—to the damping time. The picture changes when the modes are unstable. In this case the frequencies are purely imaginary; i.e. there is no oscillation and the modes grow exponentially with time [39,40].

IV. NUMERICAL RESULTS

A. Solitons

The background soliton solutions have been obtained in [31]. These solutions are topologically nontrivial, and the integer n that occurs in the boundary condition for the Skyrme field at the origin $F_{x=0} = n\pi$ is interpreted as the baryon number. Once n is fixed, the soliton solutions obtained in [31] are labeled by the values of the shooting parameters $F'_{x=0}$ and $\Phi_{x=0}$, where the index $(\ldots)_{x=0}$ refers to the value of the function calculated at the origin $x = 0$. An example of the $F'_{x=0}(a)$ and $\Phi_{x=0}(a)$ phase diagrams, presenting sequences of soliton solutions for $n = 1$, is shown in Fig. 1. From the figure it can be seen that the solutions are divided into two branches—the so-called upper and lower branches—and the two branches merge
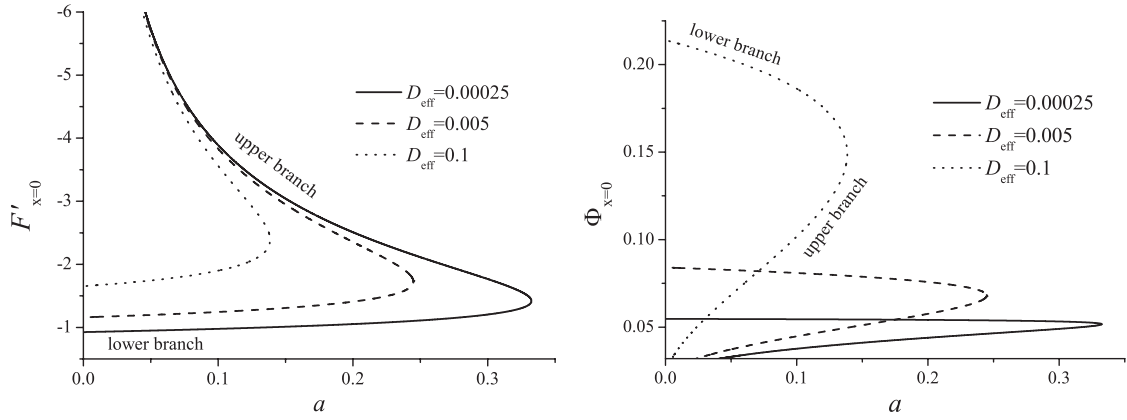
FIG. 1.   The $F'_{x=0}(a)$ and $\Phi_{x=0}(a)$ phase diagrams for sequences of soliton solutions for $n = 1$ and different values of D_{eff}.
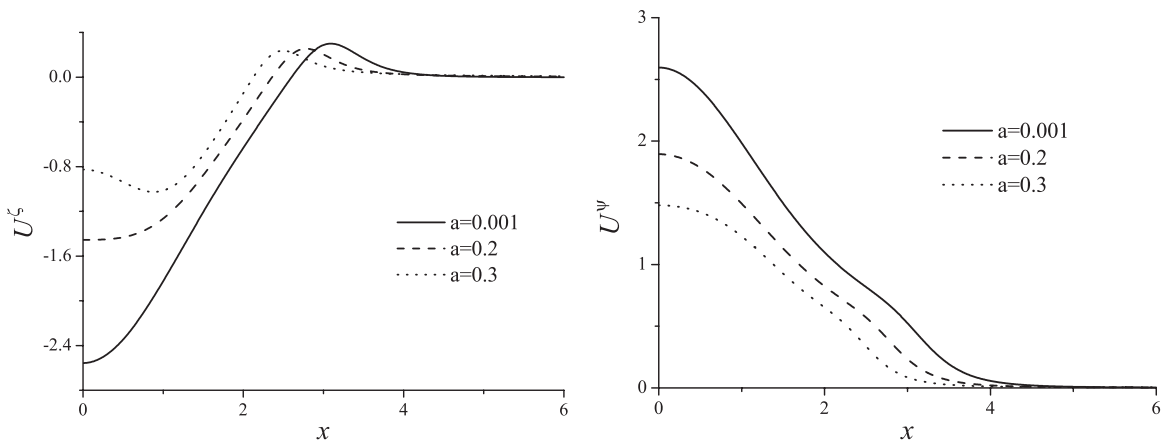

FIG. 2.   The potentials U^ζ and U^Ψ of the lower-branch solitons for $D_{\text{eff}} = 0.000\,25$ and for several values of a.

at some critical value of the parameter a_{crit}.[4] Their stability is described below.

We will start with the lower branch of solutions which is stable for ES solitons, i.e. in the case without a scalar field. The so-called potentials defined by Eqs. (33) are given in Fig. 2 for some of the soliton solutions which belong to the lower branch in Fig. 1. As it can be seen, the potential U^Ψ is positive and cannot lead to instabilities, but U^ζ is negative near the origin which means that unstable modes could exist. The asymptotic value at infinity of U^ζ is zero, and for the chosen parameters, U^Ψ tends to $U^{\Psi\infty} = -0.003\,46$ which means that the mass of the scalar field is $m = 0.0589$ and the period of the oscillation of the tail is $T = 107$ according to Eq. (37).

We evolve the coupled wave equations (28) and (29) with the appropriate QNM boundary conditions—the perturbations should be regular at the origin $x = 0$ (i.e. in our

case $\zeta_{x=0} = 0$ and $\Psi_{x=0} = 0$) and have the form of an outgoing wave at infinity. It turns out that all of the studied solutions which belong to the lower branch are stable against the considered perturbations. The time evolution of a Gaussian initial perturbation is presented in Fig. 3. The wave form consists of quasinormal oscillations in early times and an oscillatory tail for late times, where the period of the tail oscillations is the same as the period predicted by Eq. (37) within numerical errors.

Now let us consider the upper branch of soliton solutions which is unstable for the ES solitons. The two potentials U^ζ and U^Ψ are shown in Fig. 4. Again U^Ψ is positive and U^ζ is negative near the origin, but on this branch the negative part is deeper than on the lower branch. This may lead to instabilities in the wave equation for ζ, which will also affect the perturbations of the scalar field Ψ through the coupling terms. When we evolve Eqs. (28) and (29), it turns out that all of the studied upper-branch solutions are unstable. The time evolution of a Gaussian initial perturbation is presented in Fig. 5. As it can be seen, the perturbations ζ and Ψ grow exponentially with time; i.e. the QNM frequencies are purely imaginary.

---

[4]There is a discrete infinite series of copies of these branches corresponding to higher excitations with $n > 0$ [31], but they will not be discussed here since they are energetically unstable [13,17].
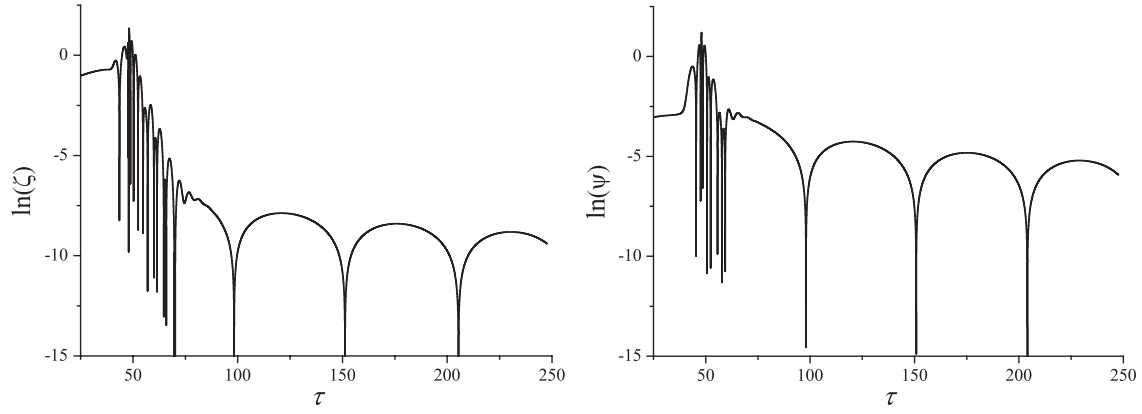
FIG. 3.   The time evolution of the perturbations ζ and Ψ of a lower-branch soliton solution with $D_{\mathrm{eff}} = 0.000\,25$ and $a = 0.2$.
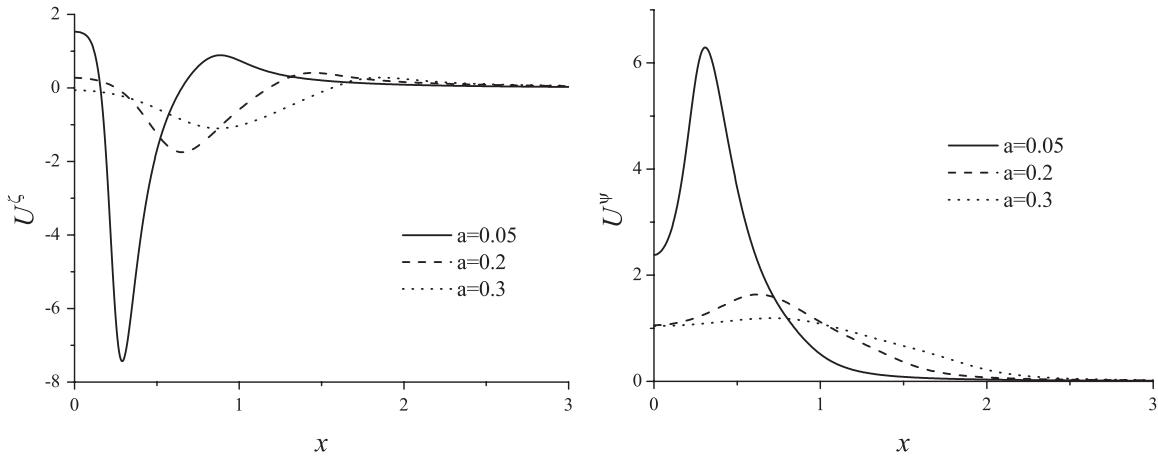

FIG. 4.   The potentials U^ζ and U^Ψ of the upper-branch solitons for $D_{\mathrm{eff}} = 0.000\,25$ and for several values of a.
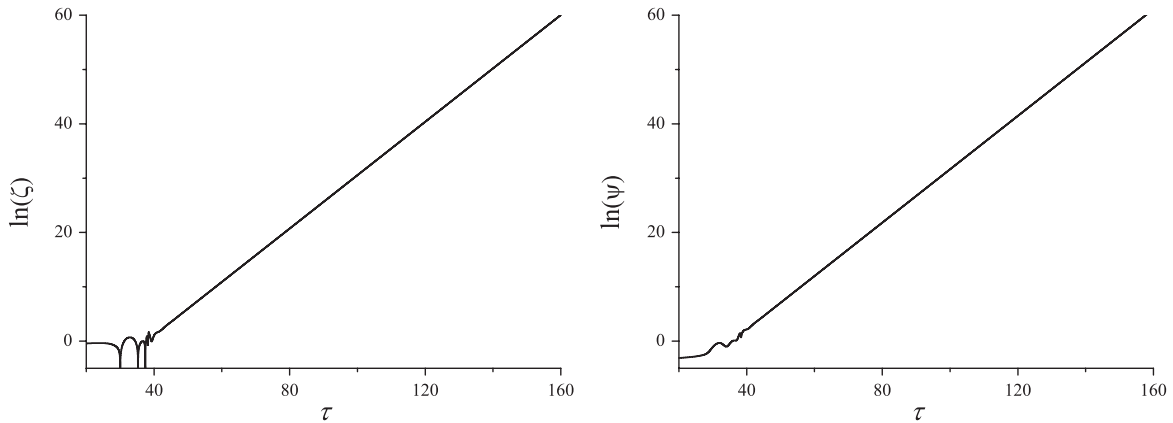

FIG. 5.   The time evolution of the perturbations ζ and Ψ of an upper-branch soliton solution with $D_{\mathrm{eff}} = 0.000\,25$ and $a = 0.2$.

The calculated frequencies for both of the branches are shown in Fig. 6. The error of the obtained frequencies is big and can reach up to 20% in some cases. The reason for this is the more complicated wave form which is due to the coupling of the wave equations and the presence of a mass term in the wave equation for the perturbations of the scalar field Ψ. Also, the background solutions are known only numerically, which is an additional
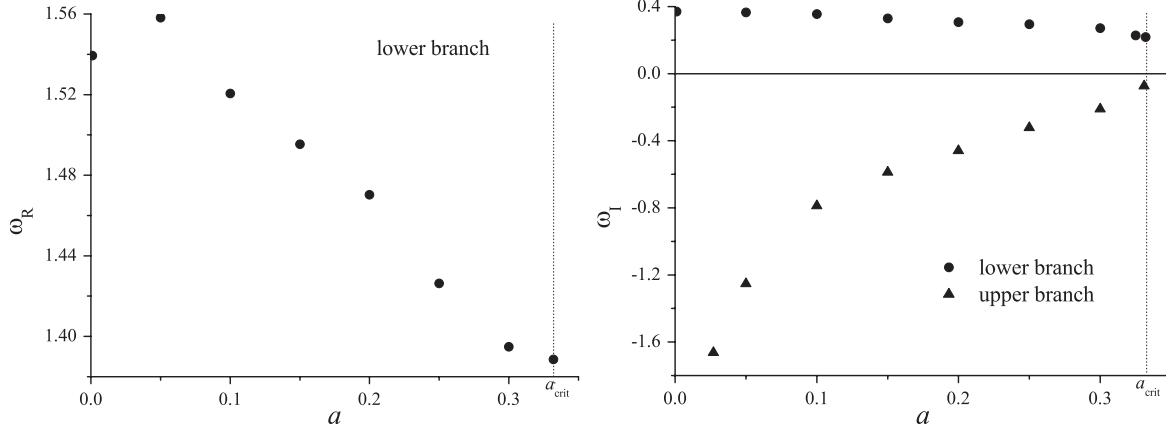
FIG. 6.   The real (left panel) and the imaginary (right panel) parts of the frequencies as a function of the parameter a for the lower and the upper branches of soliton solutions ($D_{\text{eff}} = 0.000\,25$). The frequencies are obtained using the time evolution.
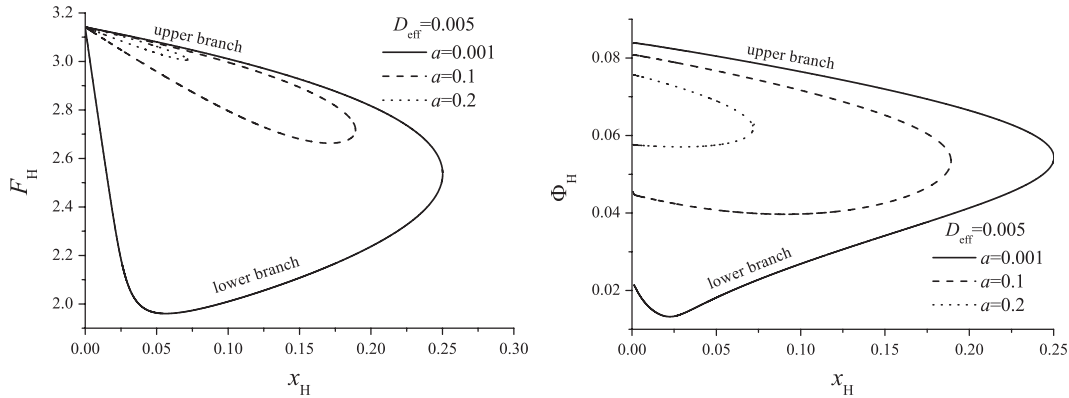

FIG. 7.   The $F_H(x_H)$ and $\Phi_H(x_H)$ phase diagrams for sequences of black-hole solutions for $D_{\text{eff}} = 0.005$ and for different values of a.

complication. But even if we take into account the error, the numerical values of the QNM frequencies differ significantly from the case without a scalar field [15] (the absolute values of the real and the imaginary parts of the QNM frequencies can be several times bigger here than in the ES case).

The qualitative behavior of the frequencies as we vary the parameter a, which is shown in Fig. 6, is the one we expected from the case without a scalar field [15]. When we increase the value of the parameter a, the real ω_R and the imaginary ω_I parts of the frequencies of the stable lower branch decrease, while the frequencies ω_I of the unstable modes of the upper branch increase (as we already said, $\omega_R = 0$ for the unstable upper branch). In the limit $a \rightarrow a_{\text{crit}}$ (i.e. when we approach the value of the parameter a where the two branches merge), the ω_I of the upper and the lower branches tend to zero; i.e. they indicate a stability change.

When we increase the value of the parameter D_{eff}, the errors of the obtained QNM frequencies increase mainly because the background solutions become more difficult to

obtain and the change in the frequencies as we vary D_{eff} is within numerical errors.

B. Black holes

Because of the presence of an event horizon, the Skyrme black holes are topologically trivial. The shooting parameters for the background black-hole solutions are the values of the Skyrmion and the scalar fields at the horizon x_H—F_H and Φ_H, respectively. The $F_H(x_H)$ and $\Phi_H(x_H)$ phase diagrams for sequences of black-hole solutions, obtained in [31], are shown in Fig. 7. As we can see, again two branches of solutions exist (upper and lower) which merge at some critical value of the radius of the horizon r_{Hcrit}.[5] The stability of the two branches is described below.

---

[5]The upper and the lower branch are defined using the $F_H(x_H)$ diagram. This is obviously different from the soliton case, and actually, the upper branch for black holes will have properties (such as stability and finiteness/divergency of some of the functions as $a \rightarrow 0$) similar to the lower branch for solitons and vice versa.
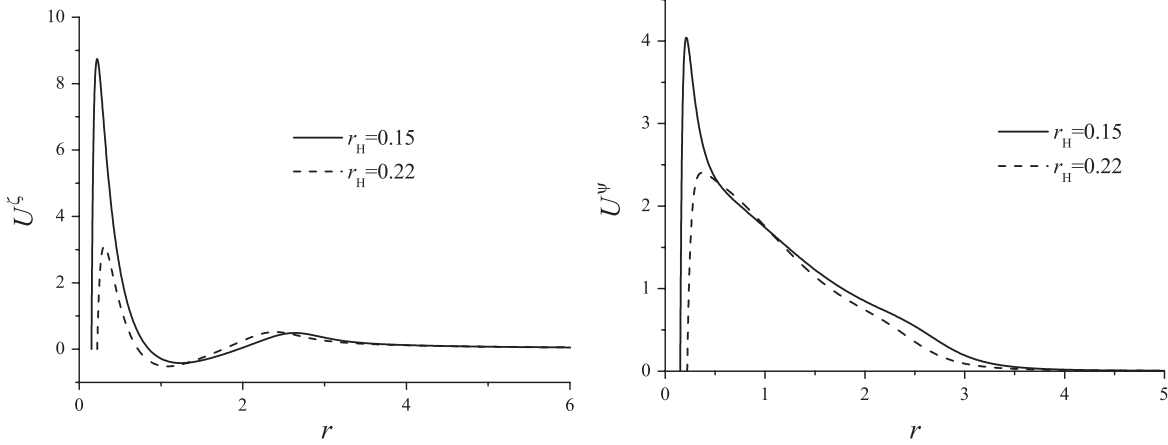
FIG. 8.   The potentials U^ζ and U^Ψ of the upper-branch black holes for $D_{\text{eff}} = 0.000\,25$ and for $a = 0.1$.
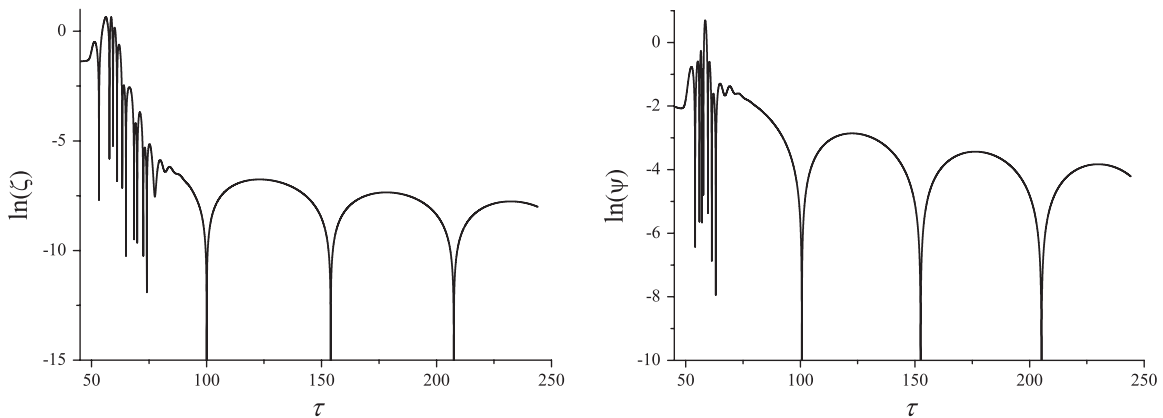

FIG. 9.   The time evolution of the perturbations ζ and Ψ of an upper-branch black-hole solution with $D_{\text{eff}} = 0.000\,25$, $a = 0.1$, and $r_H = 0.1$.

We will start with the upper branch which is stable for the ES black holes, i.e. in the case without a scalar field. The potentials U^ζ and U^Ψ for some of the upper-branch solutions are given in Fig. 8. Similar to the soliton case, the potential U^Ψ is positive and U^ζ has a negative minimum near the horizon. We evolve Eqs. (31) and (32) with the standard boundary conditions—purely ingoing waves at the horizon and purely outgoing waves at infinity. It turns out that all of the studied black holes of the upper branch are stable against the considered perturbations, and the time evolution of a Gaussian perturbation is shown in Fig. 9. Again, two stages of the time evolution are observed—the quasinormal ringing and the oscillatory tail with a period given by Eq. (37).

The potentials U^ζ and U^Ψ for some of the solutions which belong to the lower branch are shown in Fig. 10.[6] U^Ψ is again positive but U^ζ has a negative minimum near the horizon which is much deeper here than for the corre-

sponding black holes of the upper branch, which could lead to instabilities. Indeed, the time evolution shows that all of the solutions of the lower branch are unstable. The logarithms of the wave functions are shown in Fig. 11, where both ζ and Ψ grow exponentially with time.

The corresponding QNM frequencies for the upper and the lower branches are shown in Fig. 12. The error is again big (can reach up to 20%) but we can comment on the qualitative behavior of the frequencies. The real and the imaginary parts of the stable upper-branch frequencies decrease when we approach the critical value $x_{H\,\text{crit}}$ where the two branches merge. On the lower branch, which is unstable, the imaginary part of the frequencies increases when we increase x_H ($\omega_R = 0$ for this branch). So, on both branches, in the limit $x_H \rightarrow x_{H\,\text{crit}}$, the imaginary parts of the frequencies ω_I become zero; i.e. a change of stability is observed.

As discussed in [31], the properties of the black-hole solutions when we vary a for fixed x_H are similar to those of the solitons—two branches of black holes exist which merge at some critical value of the parameter a_{crit}. The

---

[6]The lower branch is unstable for the ES black holes, i.e. in the case without a scalar field.
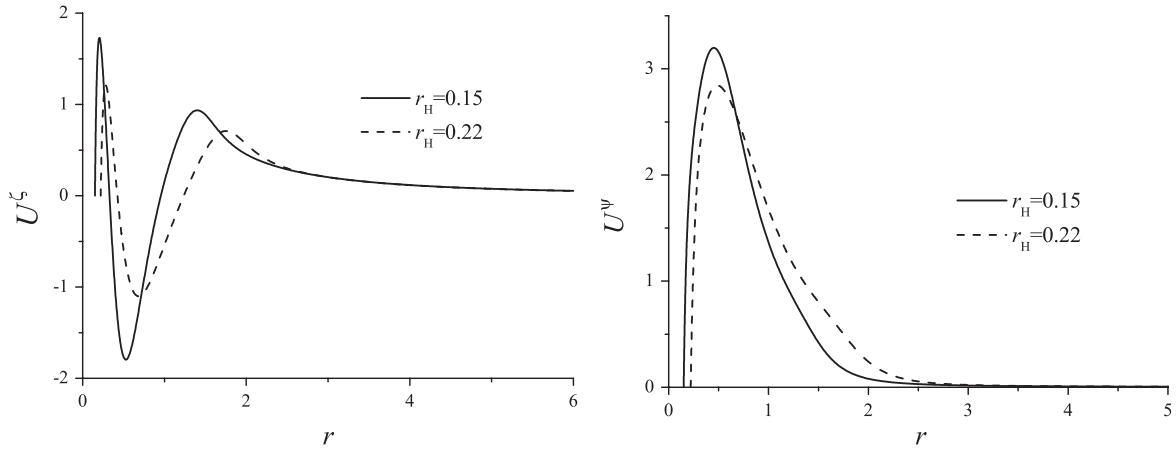
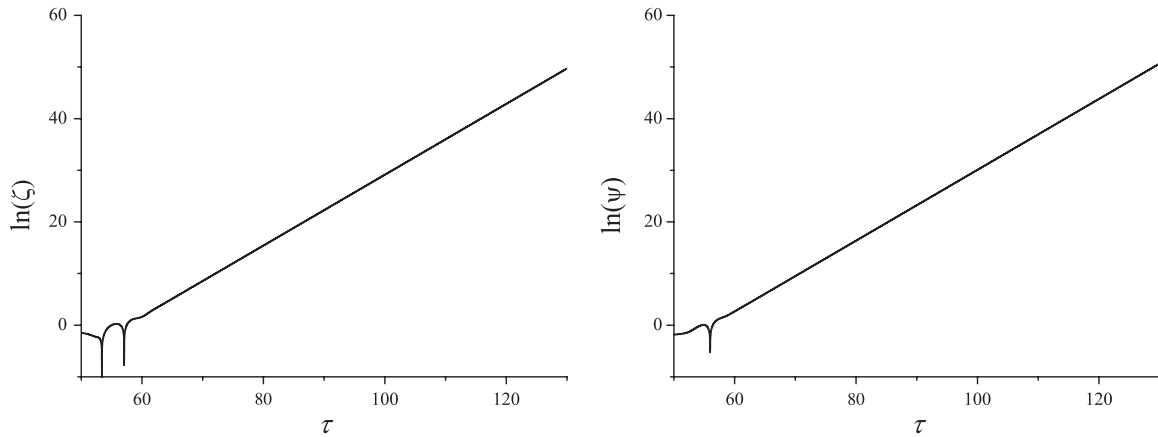FIG. 10.   The potentials U^ζ and U^Ψ of the lower-branch black holes for $D_{\text{eff}} = 0.000\,25$ and for $a = 0.1$.

FIG. 11.   The time evolution of the perturbations ζ and Ψ of a lower-branch black-hole solution with $D_{\text{eff}} = 0.000\,25$, $a = 0.1$, and $r_H = 0.1$.
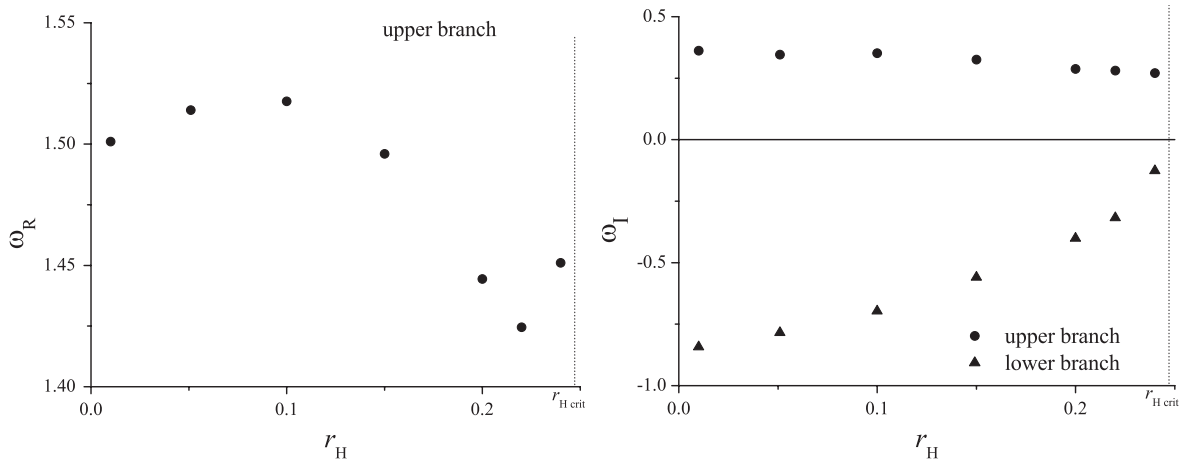

FIG. 12.   The real (left panel) and the imaginary (right panel) parts of the frequencies as a function of the radius of the horizon x_H for the lower and the upper branches of black-hole solutions ($D_{\text{eff}} = 0.000\,25$ and $a = 0.1$). The frequencies are obtained using the time evolution.

behavior of the QNM frequencies is also similar to the one shown in Fig. 6 for the soliton case. With the increase of the parameter a the real and the imaginary parts of the frequencies of the stable branch decrease, and the imaginary part of the frequencies of the unstable branch increases. The imaginary parts of both the stable and the unstable branches of black holes tend to zero when a_{crit} is approached. Similar to the soliton case, the change in the frequencies when D_{eff} varies is within numerical errors.

V. SUMMARY OF THE RESULTS

As the results indicate, the dilaton does not change the stability of the solutions. Again, the so-called lower branch of solitons is stable against radial perturbations while the upper is unstable. For the black holes the upper branch is stable and the lower is unstable. The thermodynamical stability analysis of the black holes presented in [31], which is based on the turning point method, is also in agreement with the results from the linear stability analysis.

The modes of the unstable solutions are purely imaginary, i.e. $\omega_R = 0$ and $\omega_I < 0$. The modes of the stable solutions are damped oscillations with $\omega_R \neq 0$ and $\omega_I > 0$. Hence, at the point of stability change, both the imaginary part and the real part of the QNM frequencies become zero. The time evolution of the black-hole

solutions in the vicinity of the point where the two branches merge could not be studied accurately, but still the results presented in Figs. 6 and 12, for the solitons and the black holes, respectively, show the expected qualitative behavior. Also, the numerical values of the QNM frequencies can be significantly different from the case without a scalar field; i.e. the presence of a scalar field significantly alters the spectrum quantitatively.

One more interesting observation can be made. If we consider the evolution of a test scalar field on both black-hole and soliton backgrounds, it turns out that all of the modes are damped; i.e. they are stable for both branches—the stable and the unstable ones. Thus the time evolution of the test scalar field cannot be used to study the stability of the branches.

APPENDIX: COEFFICIENTS IN THE WAVE EQUATIONS

The coefficients in the wave equations (28) and (29) are

$$A_1 = \frac{\chi_0' - \alpha_0'}{2}\frac{u_{0F}F_0'}{u_0} - \frac{a}{x}e^{\alpha_0}v_{0F}F_0' - \frac{a^2}{2x^2}e^{\alpha_0}u_0v_0F_0'^2 - \frac{1}{2}\frac{\chi_0' - \alpha_0'}{2}\frac{u_0'}{u_0} + \frac{a}{2}e^{\alpha_0}u_0F_0'^2\tilde{V}_0 + \frac{u_{0F}'F_0'}{u_0} + \frac{u_{0F}F_0''}{u_0}$$
$$+ \frac{1}{4}\frac{u_0'^2}{u_0^2} - \frac{1}{2}\frac{F_0'^2 u_{0FF}}{u_0} - \frac{1}{2}e^{\alpha_0}\frac{v_{0FF}}{u_0} - \frac{1}{2}\frac{u_0''}{u_0} + \frac{a}{x^2}e^{\alpha_0}u_0F_0'^2, \tag{A1}$$

$$A_2 = \frac{u_{0\Phi}F_0'}{x\sqrt{u_0}}, \tag{A2}$$

$$A_3 = -\frac{1}{2}e^{\alpha_0}\frac{v_{0F\Phi}}{x\sqrt{u_0}} + \frac{\chi_0' - \alpha_0'}{2}\frac{u_{0\Phi}}{x\sqrt{u_0}}F_0' - \frac{u_{0\Phi}}{x^2\sqrt{u_0}}F_0' - \frac{1}{2}\frac{u_{0F\Phi}}{x\sqrt{u_0}}F_0'^2 - \frac{1}{2}a\tilde{N}e^{\alpha_0}\frac{v_{0F}}{\sqrt{u_0}}\Phi_0' + a\tilde{N}e^{\alpha_0}\frac{\sqrt{u_0}F_0'\Phi_0'}{x}$$
$$- \frac{a}{2x^2}e^{\alpha_0}v_{0\Phi}\sqrt{u_0}F_0' + \frac{1}{2}a\tilde{N}xe^{\alpha_0}\sqrt{u_0}\tilde{V}_0F_0'\Phi_0' + \frac{u_{0\Phi}}{x\sqrt{u_0}}F_0'' + \frac{1}{2}e^{\alpha_0}\sqrt{u_0}\tilde{V}_{0\Phi}F_0' - \frac{a^2\tilde{N}}{2x}e^{\alpha_0}\sqrt{u_0}v_0F_0'\Phi_0' + \frac{u_\Phi'}{\sqrt{u_0}x}F_0', \tag{A3}$$

$$B_1 = -\frac{1}{2}\frac{e^\alpha v_{0\Phi\Phi}}{\tilde{N}x^2} - \frac{\chi_0' - \alpha_0'}{2x} - \frac{1}{2}\frac{u_{0\Phi\Phi}}{\tilde{N}x^2}F_0'^2 + xe^\alpha\tilde{V}_{0\Phi}\Phi_0' + \frac{1}{2}\frac{e^\alpha\tilde{V}_{0\Phi\Phi}}{a\tilde{N}} + a\tilde{N}e^\alpha\Phi_0'^2$$
$$- \frac{ae^\alpha v_{0\Phi}}{x}\Phi_0' - \frac{a^2\tilde{N}}{2}e^\alpha v_0\Phi_0'^2 + \frac{a\tilde{N}}{2}x^2e^\alpha\tilde{V}_0\Phi_0'^2, \tag{A4}$$

$$B_2 = -\frac{u_{0\Phi}}{\tilde{N}x\sqrt{u_0}}F_0', \tag{A5}$$

$$B_3 = \frac{1}{2}\frac{\sqrt{u_0}e^\alpha \tilde{V}_{0\Phi}}{\tilde{N}}F_0' - \frac{a^2}{2}\frac{e^\alpha v_0\sqrt{u_0}}{x}F_0'\Phi_0' + \frac{ae^\alpha\sqrt{u_0}}{x}F_0'\Phi_0' - \frac{1}{2\tilde{N}}\frac{u_{0F\Phi}}{x\sqrt{u_0}}F_0'^2 - \frac{a}{2\tilde{N}}\frac{e^\alpha v_{0\Phi}\sqrt{u_0}}{x^2}F_0' - \frac{1}{2\tilde{N}}\frac{e^\alpha v_{0F\Phi}}{x\sqrt{u_0}}$$

$$+ \frac{a}{2}xe^\alpha \tilde{V}_0\sqrt{u_0}F_0'\Phi_0' - \frac{a}{2}\frac{e^\alpha v_{0F}}{\sqrt{u_0}}\Phi_0' + \frac{1}{2\tilde{N}}\frac{u_{0\Phi}u_0}{xu_0^{3/2}}F_0', \tag{A6}$$

and the coefficients in Eqs. (31) and (32) are

$$\tilde{A}_1 = e^{\chi_0-\alpha_0}A_1, \qquad \tilde{A}_2 = e^{(\chi_0-\alpha_0)/2}A_2, \qquad \tilde{A}_3 = e^{\chi_0-\alpha_0}A_3, \tag{A7}$$

$$\tilde{A}_1 = e^{\chi_0-\alpha_0}A_1, \qquad \tilde{B}_2 = e^{(\chi_0-\alpha_0)/2}B_2, \qquad \tilde{B}_3 = e^{\chi_0-\alpha_0}B_3. \tag{A8}$$

[1] B. Carter, Phys. Rev. Lett. **26**, 331 (1971).
[2] D. C. Robinson, Phys. Rev. Lett. **34**, 905 (1975).
[3] P. O. Mazur, J. Phys. A **15**, 3173 (1982).
[4] G. L. Bunting, Ph.D. thesis, University of New England, 1983.
[5] M. Heusler, *Black Hole Uniqueness Theorems* (Cambridge University Press, Cambridge, England, 1996).
[6] P. Bizon, Acta Phys. Pol. B **25**, 877 (1994).
[7] T. H. R. Skyrme, Proc. R. Soc. A **260**, 127 (1961).
[8] T. H. R. Skyrme and G. E. Brown, *Selected Papers with Commentary of Tony Hilton Royle Skyrme (World Scientific Series in 20th Century Physics, V. 3)* (World Scientific Publishing, Singapore, 1994).
[9] H. Luckock and I. Moss, Phys. Lett. B **176**, 341 (1986).
[10] S. Droz, M. Heusler, and N. Straumann, Phys. Lett. B **268**, 371 (1991).
[11] M. Heusler, S. Droz, and N. Straumann, Phys. Lett. B **271**, 61 (1991).
[12] M. Heusler, S. Droz, and N. Straumann, Phys. Lett. B **285**, 21 (1992).
[13] P. Bizon and T. Chmaj, Phys. Lett. B **297**, 55 (1992).
[14] P. Bizon, T. Chmaj, and A. Rostworowski, Phys. Rev. D **75**, 121702(R) (2007).
[15] S. Zajac, Acta Phys. Pol. B **40**, 1617 (2009).
[16] S. Zajac, Acta Phys. Pol. B **42**, 249 (2011).
[17] N. Glendenning, T. Kodama, and F. Klinkhamer, Phys. Rev. D **38**, 3226 (1988).
[18] N. Shiiki and N. Sawado, Phys. Rev. D **71**, 104031 (2005).
[19] N. Shiiki and N. Sawado, Classical Quantum Gravity **22**, 3561 (2005).
[20] B. Kleihaus, J. Kunz, and A. Sood, Phys. Lett. B **352**, 247 (1995).
[21] T. Tamaki, K. Maeda, and T. Torii, Phys. Rev. D **64**, 084019 (2001).
[22] I. Moss, N. Shiiki, and E. Winstanley, Classical Quantum Gravity **17**, 4161 (2000).
[23] N. Sawado, N. Shiiki, K. Maeda, and T. Torii, Gen. Relativ. Gravit. **36**, 1361 (2004).
[24] Th. Ioannidou, B. Kleihaus, and W. Zakrzewski, Phys. Lett. B **600**, 116 (2004).
[25] Th. Ioannidou, B. Kleihaus, and J. Kunz, Phys. Lett. B **635**, 161 (2006).
[26] Th. Ioannidou, B. Kleihaus, and J. Kunz, Phys. Lett. B **643**, 213 (2006).
[27] B. Piette and G. Probert, Phys. Rev. D **75**, 125023 (2007).
[28] A. A. Andrianov, V. A. Andrianov, Yu. V. Novozhilov, and V. Yu. Novozhilov, JETP Lett. **43**, 7 (1986).
[29] A. A. Andrianov, V. A. Andrianov, Yu. V. Novozhilov, and V. Yu. Novozhilov, Phys. Lett. B **186**, 401 (1987).
[30] V. Nikolaev, O. Tkachev, and V. Novozhilov, Nuovo Cimento Soc. Ital. Fis. A **107**, 2673 (1994).
[31] D. Doneva, I. Stefanov, and S. Yazadjiev, Phys. Rev. D **83**, 124007 (2011).
[32] S. Hod and T. Piran, Phys. Rev. D **58**, 044018 (1998).
[33] H. Koyama and A. Tomimatsu, Phys. Rev. D **63**, 064032 (2001).
[34] H. Koyama and A. Tomimatsu, Phys. Rev. D **64**, 044014 (2001).
[35] R. Moderski and M. Rogatko, Phys. Rev. D **64**, 044024 (2001).
[36] L. E. Simone and C. M. Will, Classical Quantum Gravity **9**, 963 (1992).
[37] A. Ohashi and M. Sakagami, Classical Quantum Gravity **21**, 3973 (2004).
[38] R. A. Konoplya and A. V. Zhidenko, Phys. Lett. B **609**, 377 (2005).
[39] D. D. Doneva, S. S. Yazadjiev, K. D. Kokkotas, and I. Zh. Stefanov, Phys. Rev. D **82**, 064030 (2010).
[40] K. S. Thorne, in *Theoretical Principles in Astrophysics and Relativity*, edited by N. R. Lebowitz, W. H. Reid, and P. O. Vandervoort (The University of Chicago Press, Chicago, 1978).